THE JOURNAL OF BIOLOGICAL CHEMISTRY
Vol. 276, No. 31, Issue of August 3, pp. 28789–28798, 2001
Printed in U.S.A.

Osmolytes Stabilize Ribonuclease S by Stabilizing Its Fragments S Protein and S Peptide to Compact Folding-competent States*

Received for publication, March 2, 2001, and in revised form, May 22, 2001
Published, JBC Papers in Press, May 23, 2001, DOI 10.1074/jbc.M101906200

Girish S. Ratnaparkhi‡§¶ and Raghavan Varadarajan§‖**

From the ‡National Center for Biological Sciences, Bangalore 560 065, the §Molecular Biophysics Unit, Indian Institute of Science, Bangalore 560 012, and the ‖Chemical Biology Unit, Jawaharlal Nehru Center for Advanced Scientific Research, Jakkur P. O., Bangalore 560 064, India

Osmolytes stabilize proteins to thermal and chemical denaturation. We have studied the effects of the osmolytes sarcosine, betaine, trimethylamine-*N*-oxide, and taurine on the structure and stability of the protein·peptide complex RNase S using x-ray crystallography and titration calorimetry, respectively. The largest degree of stabilization is achieved with 6 M sarcosine, which increases the denaturation temperatures of RNase S and S pro by 24.6 and 17.4 °C, respectively, at pH 5 and protects both proteins against tryptic cleavage. Four crystal structures of RNase S in the presence of different osmolytes do not offer any evidence for osmolyte binding to the folded state of the protein or any perturbation in the water structure surrounding the protein. The degree of stabilization in 6 M sarcosine increases with temperature, ranging from −0.52 kcal mol^{-1} at 20 °C to −5.4 kcal mol^{-1} at 60 °C. The data support the thesis that osmolytes that stabilize proteins, do so by perturbing unfolded states, which change conformation to a compact, folding competent state in the presence of osmolyte. The increased stabilization thus results from a decrease in conformational entropy of the unfolded state.

Osmolytes are molecules used in nature to protect organisms against stresses of high osmotic pressure. These compounds have also been found to stabilize the native state of proteins relative to the unfolded state. The mechanism of this stabilization is not completely understood (1–4), although it is believed to result primarily from an unfavorable free energy of interaction between the osmolyte and the unfolded state of the protein (5, 6). Proteins retain activity in the presence of osmolytes suggesting that native state structure and dynamics are not greatly perturbed. However, there is little high resolution structural information available for proteins in the presence of osmolytes. The main classes of osmolytes are sugars, methyl ammonium derivatives, polyhydric alcohols, and amino acids and their derivatives (1). Molar concentrations of all the above classes of molecules have been shown to stabilize proteins. Many organisms accumulate osmolytes under conditions of water stress, such as high salinity, desiccation or freezing. *In vivo*, amino acid derivatives also counteract the accumulation of urea, which is capable of denaturing proteins. Marine cartilaginous fishes use, as osmolytes, a combination of urea and methylamines, *i.e.* a denaturant and a stabilizer, in a 2:1 ratio (1, 7, 8). Stability studies on RNase T1, RNase A, and other proteins have shown that, if the 2:1 ratio of urea:methylamine is maintained, the methylamine is able to counteract the destabilizing effect of the denaturant (1, 7, 8).

In an effort to further our understanding of the basis of osmolyte stabilization of proteins, we have studied the stabilization of the fragment complementation system ribonuclease S (RNase S)[1] in four structurally similar osmolytes, namely sarcosine, betaine, trimethylamine-*N*-oxide (TMAO), and taurine. RNase S is a complex of two fragments, the N-terminal S peptide (S pep; residues 1–20) and the C-terminal S protein (S pro; residues 21–124). The fragments form a 1:1 complex in solution, and RNase S has properties similar to its parent molecule RNase A, in terms of structure (9), activity as well as dynamics (10). A large number of crystal structures of RNase A, RNase S (9), and a number of mutants of RNase S (11, 12) have been solved to a high resolution. Both fragments of RNase S have been extensively studied. S pep has been studied as a system to understand helicity in a polypeptide chain (13, 14). S pro is unusual in terms of its folded, stable structure despite being a fragment of a natural protein (10, 15). Although S pro is only 104 amino acids long, direct structural characterization by two-dimensional NMR has not been possible because of the tendency of S pro to aggregate at the millimolar concentrations required for NMR studies. S pro has also not been crystallized. Native state concentration-dependent hydrogen exchange studies using two-dimensional NMR have been used to get indirect information on the structure of S pro in its free state (10).

The binding of S pep to S pro is one of the last steps in the folding pathway of RNase A (16) and the S pro·S pep interaction is a model system to study protein folding and stability (12, 17, 18). In the present work we have examined the effects of

* This work was supported by grants from the Council of Scientific and Industrial Research, the Department of Science and Technology, and the Department of Biotechnology (India) (to R. V.). The costs of publication of this article were defrayed in part by the payment of page charges. This article must therefore be hereby marked "*advertisement*" in accordance with 18 U.S.C. Section 1734 solely to indicate this fact.

The atomic coordinates and structure factors (code 1J7Z, 1J80, 1J81, and 1J82) have been deposited in the Protein Data Bank, Research Collaboratory for Structural Bioinformatics, Rutgers University, New Brunswick, NJ (http://www.rcsb.org/).

¶ Present address: the Chemistry and Biochemistry Dept., University of California at Los Angeles, CA 90095.

** A recipient of a Senior Research Fellowship from the Wellcome Trust and a Swarnajayanthi Fellowship from the Government of India. To whom correspondence should be addressed: Molecular Biophysics Unit, Indian Institute of Science, Bangalore, 560 012, India. Tel.: 91-80-3092612; Fax: 91-80-3600535 or 91-80-3600683; E-mail: varadar@mbu.iisc.ernet.in.

[1] The abbreviations used are: RNase S, product of proteolytic cleavage of bond 20–21 in RNase A; RNase A, bovine pancreatic ribonuclease; r.m.s.d., root mean square deviation; Nle, norleucine; MC, main chain; SC, side chain; *B*-factor, crystallographic atomic temperature factor; S pro, S protein; S pep, S peptide; T_m, temperature at which fraction of unfolded protein is 0.5; MP, mean normalized packing value; OS, occluded surface; DSC, differential scanning calorimetry; TMAO, trimethylamine-*N*-oxide; BMAAC, N^{α}-benzoyl-L-arginine-7-amido-4-methylcoumarin; CD, circular dichroism.

TABLE I

Aggregation profile of S pro, RNase A, and RNase S in the presence of osmolytes after a temperature melt (see "Experimental Procedures")

Protein	Osmolyte	pH 5[a]	pH 6	pH 7	pH 8
S pro	0 M[a]	√	√	√	√
	4.5 M TMAO	√	√	xx[b]	xxx[b]
	6 M sarcosine	√	√	√	√
	4.5 M betaine	√	√	√	√
	0.6 M taurine	√	√	√	√
RNase S	0 M	√	√	√	√
	4.5 M TMAO	√	√	x[b]	xx[b]
	6 M sarcosine	√	√	√	√
	4.5 M betaine	√	√	√	√
	0.6 M taurine	√	√	√	√
RNase A	0 M	√	√	√	√
	4.5 M TMAO	√	√	√	x[b]
	6 M sarcosine	√	√	√	√
	4.5 M betaine	√	√	√	√
	0.6 M taurine	√	√	√	√

[a] Buffers: pH 5 and 6 (50 mM sodium acetate, 100 mM NaCl), pH 7 and 8 (50 mM Hepes, 100 mM NaCl).

[b] x, indicates aggregation: xxx, OD (optical density) at 450 nm between 1.0 and 0.8; xx, OD between 0.6 and 0.4; x, OD between 0.1 and 0.2; √, OD < 0.1.

osmolytes on the structure and stability of RNase S. There are several advantages of using a bimolecular fragment complementation system such as RNase S, as opposed to a monomeric protein for these studies. The effect of osmolytes on the stability of the individual fragments (models for the unfolded and partially folded states) can be studied in addition to effects on the folded complex. RNase S is easily crystallized, and the structure of RNase S can be solved in the presence of molar concentrations of denaturants (19) and osmolytes. The thermodynamics of interaction of S pep with S pro in the presence of osmolytes can be characterized using titration calorimetry as a function of temperature. Thermodynamic binding parameters (ΔG^0, ΔH^0, ΔS, and ΔC_p) can be measured accurately without extrapolation of the data from high temperature or in the presence of denaturants.

EXPERIMENTAL PROCEDURES

Materials—RNase A (type XII A), Subtilisin Carlsberg, ammonium sulfate, sarcosine, trimethylamine-*N*-Oxide (TMAO), betaine, taurine, trypsin (TPCK-treated), and N^{α}-benzoyl-L-arginine-7-amido-4-methylcoumarin (BAAMC) were purchased from Sigma Chemical Co. Stock solutions of 7 M sarcosine, 5 M betaine, 5 M TMAO, and 0.8 M taurine were made in MilliQ water, based on the solubility of each osmolyte. RNase S was prepared by subtilisin digestion of RNase A and was purified using a 1-ml Resource S column (20). S pro was prepared, purified, and quantitated as described previously (10).

pH Dependence of Osmolyte Stability—The reversibility of thermal denaturation for RNase A, RNase S, and S pro was studied as a function of pH and osmolyte to decide upon the experimental conditions for measurement of protein thermal stability. The S pro fragment at high concentrations (>1 mM) has a tendency to aggregate and precipitate near its isoelectric point (pI = 8.3). Osmolytes were mixed with protein at a single, high concentration of osmolyte (6 M sarcosine, 4.5 M TMAO, 4.5 M betaine, and 0.7 M taurine) at four different pH values (pH 5, 6, 7, and 8). The buffers used were 50 mM sodium acetate, 100 mM NaCl at pH 5 and 6, and 50 mM Hepes, 100 mM NaCl at pH 7 and 8. Insoluble aggregation of protein (final concentration of 30 μM) was checked by scanning the solution (150 μl final volume) in a Bio-Rad 450 Microplate reader at 450 nm. S pro showed visible aggregation (see Table I) at 20 °C when added to a final concentration of 4.5 TMAO at pH 8. All solutions were transferred to Eppendorf tubes, which were heated in a heating block containing water to 90 °C over a period of 60 min. The solutions were allowed to cool slowly to 20 °C and transferred back to the enzyme-linked immunosorbent assay plate, and the aggregation of protein was checked once again. Heating and cooling seemed to enhance the aggregation of S pro in TMAO at pH 8, and aggregation was also seen at pH 7. S pro did not show visible precipitation in buffer alone under these experimental conditions. Visible aggregates were also seen in RNase S at pH 8, 4.5 M TMAO. RNase A, at pH 8, 4.5 M TMAO, also showed aggregation but to a very small extent. Apart from the conditions referred to above, no other well showed significant aggregation of protein. Based on the aggregation profile (Table I) of S pro, RNase S, and RNase A at different pH values, we chose to study the stabilization of the proteins in 100 mM sodium chloride, 50 mM sodium acetate at pH 5. This buffer is used for all further experiments unless indicated otherwise.

Spectra and Temperature Melts—Circular dichroic (CD) spectra were collected in a JASCO J720 spectrometer using a cuvette of 1-mm path length. The final concentrations of osmolytes used were 6, 4.5, 3, and 1 M. The 6 M data could be collected only for sarcosine, and data for taurine were collected at a single concentration of 0.5 M. Spectra were collected in the wavelength range of 300–235 nm with a protein concentration of 200 μM for RNase A, RNase S, and S pro. Spectra could not be collected below 235 nm because of the high absorbance of molar concentrations of osmolyte. The temperature denaturation studies (T_m) were done using a peltier cell in the temperature range 10–90 °C. Unfolding was monitored by the CD signal at 239 nm using a protein concentration of 50 μM for RNase A, RNase S, or S pro. The protein concentrations were based on known molar extinction coefficients for these proteins (17, 20). RNase S was prepared by mixing S pro with a slight molar excess (1:1.1) of S pep. The S pep used in these studies was the S15 (M13Nle) peptide (21). The Nle analog was used to minimize problems associated with oxidation of Met. The T_m data was fit to a two-component-dissociating system for RNase S (22, 23) and a two-state fit for S pro and RNase A. Fluorescence spectra were collected on an SPEX fluorometer. The excitation wavelength and slit width were set at 280 nm and 0.1 mm, respectively. Emissions were monitored from 300 to 400 nm with an emission slit width of 4 mm. Each spectrum was an average of five scans. The protein concentration in the cuvette was 10 μM, and the path length used was 1 cm. The buffer was the same as that used for the CD studies.

Gel Filtration—A Superdex peptide HR 10/30 (Amersham Pharmacia Biotech) column attached to the Akta FPLC (Amersham Pharmacia Biotech) was chosen to probe the effect of osmolytes on the conformational state of RNase S and its fragments. The column has a void volume of 7.7 ml and determines the molecular mass accurately in the range 14 to 0.1 kDa. It is, therefore, suitable for characterization of RNase A, RNase S, S pro, and S pep. Minor changes in the conformation of these proteins can be measured using this column. The column was pre-equilibrated with two column volumes (50 ml) of buffer/osmolyte and then run at 20 °C at a flow rate of 0.3 ml min^{-1} in 100 mM NaCl, 50 mM sodium acetate, pH 5, with or without 3 M sarcosine. 100 μl of sample (50 μM) was injected in each run. The absorbance was monitored simultaneously at 220, 254, and 280 nm. S pep does not absorb at 280 nm. Sarcosine was chosen for these experiments, because it stabilized RNase S and S pro to a significant extent at 3 M, the maximal concentration at which we could work at a reasonable back pressure and flow rate.

Trypsin Cleavage—Proteolytic cleavage of proteins has been used as a probe of protein conformation and stability (20, 24). RNase A is resistant to tryptic cleavage at room temperature, but RNase S and S pro are sensitive to tryptic cleavage (25). The solution conditions for tryptic cleavage of RNase S and S pro have been described in detail earlier (20). Cleavage was done at a single concentration of protein (0.1 mM) in 10 mM HEPES, 1 mM $CaCl_2$, pH 8.0, 20 °C. Trypsin was used at a final concentration of 0.1 mg ml^{-1} in the absence and 0.2 mg ml^{-1} in the presence of 6 M sarcosine (see "Results"). To separate the effect of the osmolyte (6 M sarcosine) on S pro/RNase S from the effect of

TABLE II
Data collection and refinement details of the experimental and control data sets

Data	Cell		R_{merge}[a]	No. of Refl	Res[b]	Number of waters	R	R_{free}	r.m.s.d. bond	
	$a=b$	c							Length	Angle
	Å		%		Å					
Control-1[c]	44.66	97.99	6.4	8608	1.9	46	20.9	25	0.006	1.5
Control-2	44.61	97.98	6.6	8560	1.9	50	20.7	24	0.005	1.5
2 M sarcosine	44.59	98.00	11.1	6172	2.1	43	20.7	27	0.007	1.2
2 M TMAO	44.67	97.65	7.6	5300	2.2	39	21.0	25	0.007	1.2
2 M betaine	44.60	98.14	7.2	5378	2.1	41	20.4	27	0.007	1.1
0.5 M taurine	44.96	97.83	8.9	3955	2.3	39	18.9	27	0.005	1.2

[a] R_{merge} is defined as $100 \times \Sigma|I_h - \langle I\rangle|/\Sigma I_h$, where I_h is the intensity of the reflection h.
[b] Completion of the data is based on the shell at which >50% of 2σ reflections are present. All reflections were used for refinement.
[c] The two control structures have been described in Ref. 19.

osmolyte on the activity and stability of trypsin itself, an assay using a fluorescent trypsin substrate (BAAMC) was done in the presence and absence of osmolyte. The assay conditions and BAAMC storage were as described previously (26). The BAAMC cleavage reaction was monitored in an SPEX fluorometer with excitation at 333 nm (slit width, 0.7 nm) and emission at 440 nm (slit width, 10 nm). The assay was carried out at both pH 7 and 8 to facilitate comparison with earlier proteolytic cleavage experiments.

Crystallization, Osmolyte Soaking, Data Collection, Refinement, and Analysis—Crystals of RNase S of size $0.7 \times 0.5 \times 0.4$ mm were obtained (9) and stored in stabilization solution (70% ammonium sulfate, 100 mM sodium acetate, pH 4.75) for a period of 1–8 weeks. RNase S crystals in 20 ml of stabilizing solution were transferred to stabilizing solutions containing increasing concentrations of the desired osmolyte in a stepwise manner by increasing the concentration of additive to the final concentration over a period of 2–3 h. Once at the final osmolyte concentration, the crystals were washed with 20 ml of solution three times (3×20 ml) and then soaked in the solution overnight (10–18 h). Crystals were stable in 2 M (but not in 2.5 M) of sarcosine, TMAO, and betaine, whereas for taurine, the crystals were unstable at any osmolyte concentration greater than 0.5 M. The data collection and refinement was done as described previously (19). Six data sets were collected. Out of these four was osmolyte-soaked crystals. The remaining two data sets (control-1 and control-2) were in the absence of osmolyte. These were collected on separate crystals but in identical solution conditions. For all six data sets identical data collection, data reduction, and refinement procedures were followed. The relevant data collection and refinement parameters are listed in Table II.

The crystal structures were analyzed by r.m.s.d. and ΔB-factor plots (19) for the protein as well as for the water shell around the protein. Parameters such as accessibility (27) and depth (28) were also analyzed. For any parameter X, the $\Delta X = X_{\text{control-2}} - X_{\text{control-1}}$ was used as the expected background change of the parameter between two identical data sets. The possibility of changes in the packing density of the polypeptide chain after soaking the crystal in osmolytes was explored by using the Occluded Surface algorithm (29) and by calculating the radius of gyration of the protein. The parameters ΔOS (per residue) and Mean Packing Value were calculated as described previously (12, 30). The Δ(Mean Normalized Packing Value) or ΔMP = Mean Normalized Packing Value of soaked structure or mutant − Mean Normalized Packing Value of control. The Normalized Mean Packing Value (29) is the average of the packing value of all residues of a protein and has been shown (30) to be a useful and sensitive parameter to quantitate the packing density of a protein.

Calorimetry—Calorimetric titrations were done on an isothermal titration calorimeter from MicroCal Inc. as previously described (12, 17, 31) in the temperature range 6–70 °C. The buffer used was 50 mM sodium acetate, 100 mM NaCl, pH 5. The thermodynamic parameters (K, ΔG^0, ΔH^0, and ΔC_p) for binding of S pep to S pro in the presence and absence of osmolytes were determined as described previously (31). Titrations above 40 °C could only be accomplished in the presence of sarcosine. In the case of TMAO and betaine, insoluble aggregation of S pro in the titration cell prevented collection of data. Differential scanning calorimetry (DSC) was done on a Microcalorimeter from MicroCal Inc. as described (32). DSC runs were done for RNase A, RNase S, and S pro under the same buffer conditions (pH 5) as the titration calorimetry at a protein concentration of 50 μM in the presence and absence of 6 M sarcosine. The Scan rate was 90 K h^{-1}, and runs were done in duplicate with multiple scans for each sample run to confirm reversibility. The S protein and RNase A scans were fit to a two-state model. The data for RNase S was fit to a dissociating system (22). Both titration calorimetry and the DSC data were analyzed using the ORIGIN package.

RESULTS

Osmolytes Stabilize RNase A, RNase S, and S Pro to Heat Denaturation—T_m in the presence of molar concentrations of osmolytes show that RNase A, RNase S, and S pro are stabilized against heat denaturation in the presence of sarcosine, betaine, and TMAO (Fig. 1*A*; Table III). The osmolytes stabilize RNase A, RNase S, and S pro to different extents, with sarcosine having the maximal stabilizing effect in all cases. These osmolytes have been shown to stabilize RNase A in previous studies (3, 7). T_m was calculated by fitting the spectroscopic data as described under "Experimental Procedures." There appears to be a linear relationship between the T_m value and the concentration of osmolyte. 0.7 M taurine stabilizes RNase A but destabilizes RNase S and S pro by 0.8 °C and 3 °C, respectively. The largest stabilization for all three systems is in the presence of 6 M sarcosine. All three proteins show reversibility to thermal denaturation in the presence or absence of sarcosine, betaine, and TMAO at pH 5.

Sarcosine Perturbs the Tertiary Structure of S Pro—Because sarcosine stabilizes all three proteins to heat denaturation by a significant amount, we monitored the effect of sarcosine and other osmolytes on the tertiary structure of RNase A, RNase S, and S pro (Fig. 1, *B* and *C*). Fig. 1*B* shows that in increasing concentrations of sarcosine the near-UV spectra show significant changes, both at 278 nm as well as 240 nm for S pro but not for RNase S and RNase A (data not shown). The increase in the ellipticity for S pro is larger than that observed for RNase S and is specially striking for the positive peak at 240 nm (marked by an asterisk). For RNase A and S, the weak positive band near 240 nm is primarily due to the disulfides (33) with a small contribution from the Tyr L*a* bands (34). The intensity of the 240-nm band increases at basic pH and at low temperature (35) for all three proteins. At pH 5 the band is not prominent in RNase A and RNase S and increases to a very small extent in the presence of osmolyte. The 240-nm band is more prominent for sarcosine than for the other osmolytes (Fig. 1*C*). The increase in intensities of the 240-nm peak with increasing sarcosine concentrations for S pro may indicate a compaction of S pro concomitant with a change in the dihedral angle of disulfides or a change in the environment of the disulfides in the presence of sarcosine. Taken together with the increase in the magnitude of the 278-nm peak, this suggests a conformational transition in S pro at higher sarcosine concentrations. As in RNase S, increasing concentrations of sarcosine result in quenching of the fluorescence spectra for S pro. At 6 M sarcosine, there is a small but perceptible shift of the fluorescence maximum from 308 to 310 nm, which indicates that the tyrosines contributing to this emission band are more exposed than in the absence of sarcosine. Far-UV-CD spectra in molar

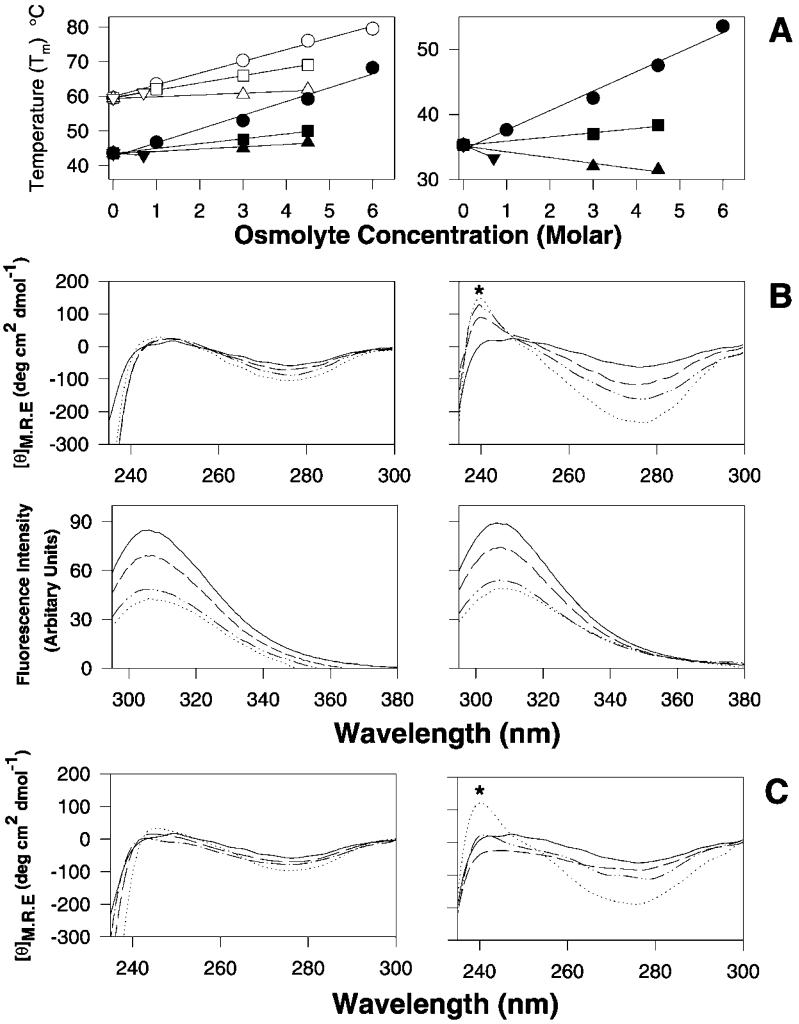

FIG. 1. **Effects of osmolytes on the stability and structure of RNase S in 100 mM NaCl, 50 mM sodium acetate, pH 5.** The *panels* on the *left* are for RNase S and those on the *right* are for S pro. *A*, T_m of RNase S and S pro at 50 μM as a function of osmolyte concentration in the presence of sarcosine (●), betaine (■), TMAO (▲), and taurine (▼). The *empty symbols* in the *panel* on the *left* indicate T_m values for RNase A. The mean residue ellipticity (θ) was monitored at 239 nm. *B*, spectra of RNase S and S pro in increasing concentrations of a single osmolyte, sarcosine. Near-UV-CD spectra at 200 μM and fluorescence spectra at 10 μM RNase S. 0 M (*solid line*), 1 M (*dashed line*), 3 M (*dashed and dotted line*), and 6 M (*dotted line*). The *asterisk* indicates the 239-nm peak for S pro in the presence of sarcosine. *C*, near-UV-CD spectra for RNase S and S pro at the same concentration of different osmolytes. 0 M (*solid line*), 4.5 M TMAO (*dashed line*), 4.5 M betaine (*dashed and dotted line*), and 4.5 M sarcosine (*dotted line*).

TABLE III

T_m values for thermal denaturation of RNase A, RNase S, and S pro at 50 μM protein using CD spectroscopy (λ = 239 nm) in 100 mM sodium chloride, 50 mM sodium acetate, pH 5

The T_m values are obtained from fits to the raw data as described under "Experimental Procedures."

Osmolyte	RNase A		RNase S		S pro	
	T_m	ΔT_m	T_m	ΔT_m	T_m	ΔT_m
			°C			
0 M control	60.2		43.6		36.1	
6 M sarcosine	80.1	19.9	68.2	24.6	53.5	17.4
4.5 M sarcosine	76.0	15.8	58.2	14.6	47.5	12.2
4.5 M TMAO	62.0	1.8	46.7	3.1	33.7	−2.4
4.5 M betaine	69.0	8.8	50.0	6.4	34.8	−1.3
0.7 M taurine	61.9	1.7	42.8	−0.8	32.3	−3.8

osmolyte concentrations could not be collected because of high absorbtion at wavelengths below 230 nm.

Effect of Sarcosine on the Stokes Radius of S Pep and S Pro—Gel filtration experiments at pH 5 indicate that S pro has a similar Stokes radius to RNase S and RNase A despite being 20 residues smaller (Fig. 2). This indicates that S pro has a less compact structure than RNase S. Despite having a less compact and relatively less stable structure, S pro has not been reported to bind 8-anilinonaphthalene sulfonate and does not show any features of a molten globule. Because S pro shows significant changes in its CD spectra at 240 nm, gel filtration experiments of S pro were carried out in the presence and absence of sarcosine. Fig. 2 shows that the peak elution volumes for RNase A and S pro in the presence (9.03 and 9.03 ml) and absence (9.00 and 9.00 ml) of 3 M sarcosine is very similar. There is a very small increase in the elution volume for each protein in the presence of sarcosine. The experiments were repeated twice in each case, and the repeats gave identical results. This may indicate that both RNase A and S pro become more compact in the presence of sarcosine. The Akta FPLC-Superdex (10/30) system is a very stable system, and in buffer the S pro peak eluted at 9.00 ± 0.009 ml for six fast-protein liquid chromatography runs. This indicates that the 0.03-ml shift may be significant, although we cannot rule out the possibility that this shift is simply a consequence of the presence of 3 M sarcosine in the column. S pep clearly has a larger elution volume (12.15 ml) in the presence of 3 M sarcosine than in its absence (11.91 ml), indicating that it became more compact in the presence of sarcosine.

Sarcosine Stabilizes S Pro against Tryptic Digestion—RNase

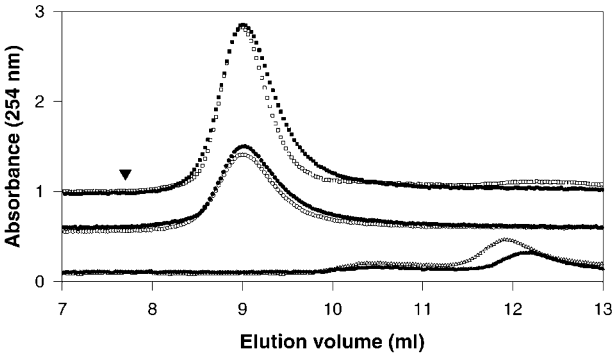

FIG. 2. **Representative traces of gel filtration of RNase A (*squares*), S pro (*circles*), and S pep (*triangles*) in the absence (*empty symbols*) and presence (*filled symbols*) of 3 M sarcosine.** The elution profiles of RNase S (data not shown) are identical to that of RNase A. The *filled inverted triangle* represents the void volume of the column.

S and S pro are sensitive to trypsin digestion (20) whereas RNase A is resistant. We have used proteolytic cleavage as a probe of protein conformation by looking at the sensitivity of the S pro to tryptic cleavage in the presence and absence of 6 M sarcosine (Fig. 3*A*). As a control, cleavage of a small molecule substrate BAAMC (see "Experimental Procedures"), was done under similar conditions in the presence or absence of 6 M sarcosine (Fig. 3*B*). The rate of BAAMC cleavage by trypsin slows down by a factor of two in the presence of 6 M sarcosine. This was tested at four enzyme concentrations and two different pH values (pH 7, 8). The rate of trypsin cleavage in 6 M sarcosine is the same as that in buffer if twice the amount of trypsin is used in the presence of 6 M sarcosine. In Fig. 3*A*, S pro digestion in the presence of 6 M sarcosine has twice the amount of trypsin in comparison to digestion in the absence of sarcosine, so that the activity of trypsin is similar in the presence or absence of 6 M sarcosine.

6 M sarcosine protects S pro (Fig. 3*A*) and RNase S (data not shown) from tryptic cleavage. Trypsin digests S pro slowly in the presence of 6 M sarcosine. Under the conditions of the experiment, protection is seen even after 3 h of digestion. The pattern of cleavage also shows that, unlike in buffer (*lanes 2–5*), in the presence of 6 M sarcosine (*lanes 7–10*) there is protection of protein fragment, which is resistant to tryptic cleavage. The molecular weight of these species is very near to that of S pro and indicates deletion of N- or C-terminal peptide by trypsin.

Trypsin can theoretically cut the S pro sequence in eleven positions (Fig. 3*C*). We used electrospray mass spectrometry to identify the protected fragment of S pro. Intact S pro was found to have a mass of 11,544 Da, in good agreement with the calculated mass of 11,542 Da expected for residues 21–124 of RNase A. After tryptic cleavage in the presence of sarcosine, S pro was reduced with 10 mM dithiothreitol and dialyzed against an excess volume of water to remove salts and small cleavage products and lyophilized. The digested and reduced S pro showed a major peak of 9569 Da in addition to the expected mass of S pro (11, 542 Da). The tryptic cleavage sites of S pro indicate that residues 38–124 of S pro have a calculated mass of 9568 Da, in good agreement with the size of the protected fragment. No other tryptic fragment of S pro has a calculated mass near 9569 Da. The protected fragment, S pro-(38–124) remains attached to the N-terminal peptide-(21–37), because of the disulfide bond between residues 26 and 84. This disulfide bond is broken by adding dithiothreitol.

The characterization of tryptic fragments of RNase A (36) and RNase S and S pro (25) have previously been worked out in some detail. These studies indicate that the N-terminal residues (residues 31–33 for S pro) are most sensitive to tryptic cleavage, and this is followed by the cleavage in the C-terminal domain in S pro (cleavage in residues 91–92 and 98–99). Our experiments indicate that S pro cleavage by trypsin is slower in the presence of sarcosine and the S pro-(38–124) fragment is protected against further cleavage. This fragment is not protected in the absence of sarcosine. This protection of the S pro fragment against tryptic digestion in combination with the CD data suggests that this region probably adopts a conformation similar to that of folded S pro (as in RNase S) in the presence of sarcosine.

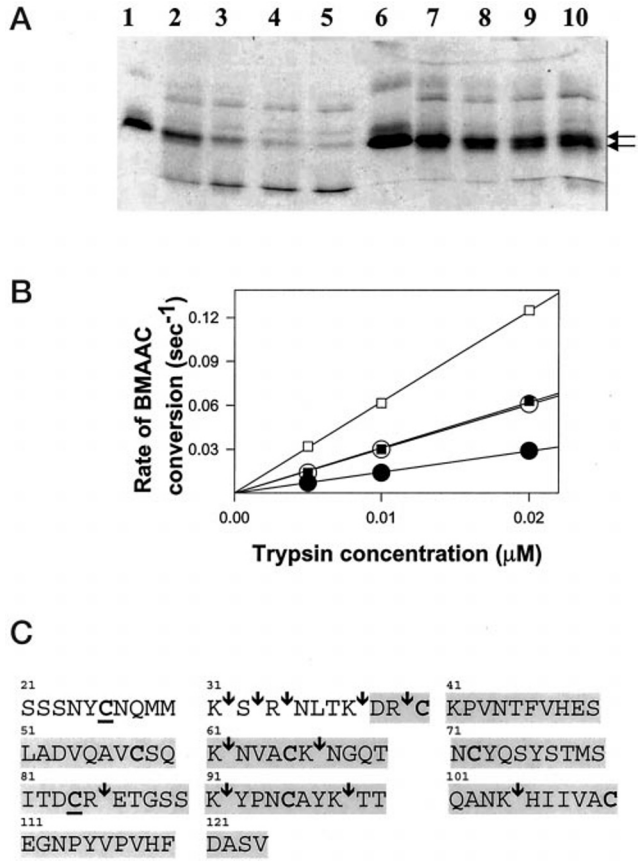

FIG. 3. **Effect of sarcosine on the tryptic cleavage of S pro.** *A*, tryptic cleavage of S pro in the absence (*lanes 1–5*) and presence (*lanes 6–10*) of 6 M sarcosine. The time points are 0, 10, 20, 30, and 60 min for each case. The *arrows* indicate the intact S pro and a protected fragment (S pro-(38–124)) in the presence of sarcosine. *B*, the effect of 6 M sarcosine on the cleavage of a fluorescent substrate of trypsin, BMAAC at pH 8 (*squares*) and pH 7 (*circles*). In the presence of 6 M sarcosine (*filled symbols*), the rate of trypsin cleavage is half of that in its absence. The rate of cleavage of substrate by trypsin is equal in the absence and presence of 6 M sarcosine if twice the concentration of trypsin is used in the presence of 6 M sarcosine. *C*, potential sites for tryptic cleavage of S pro (indicated by *arrows*). The *shaded residues* indicate the fragment protected (S pro-(38–124)) in the presence of sarcosine. The residue numbering is based on the sequence of RNase A.

Osmolyte Does Not Perturb the Crystal Structure of RNase S—The crystalline state of a protein has large empty channels, which allow molecules as large as 3000 Da to diffuse in the crystal lattice and interact with the protein (37, 38). Osmolytes should therefore diffuse into the crystal lattice and be in a position to bind protein molecules inside the crystal lattice. RNase S crystals have previously been soaked with substrates (39) and denaturants (19). RNase S is enzymatically active in the crystalline state (39). Soaking of crystals is a useful tool to probe the effect of small ligands and solvent perturbants on crystals of a protein.

RNase S crystals were soaked in all four osmolytes but at a

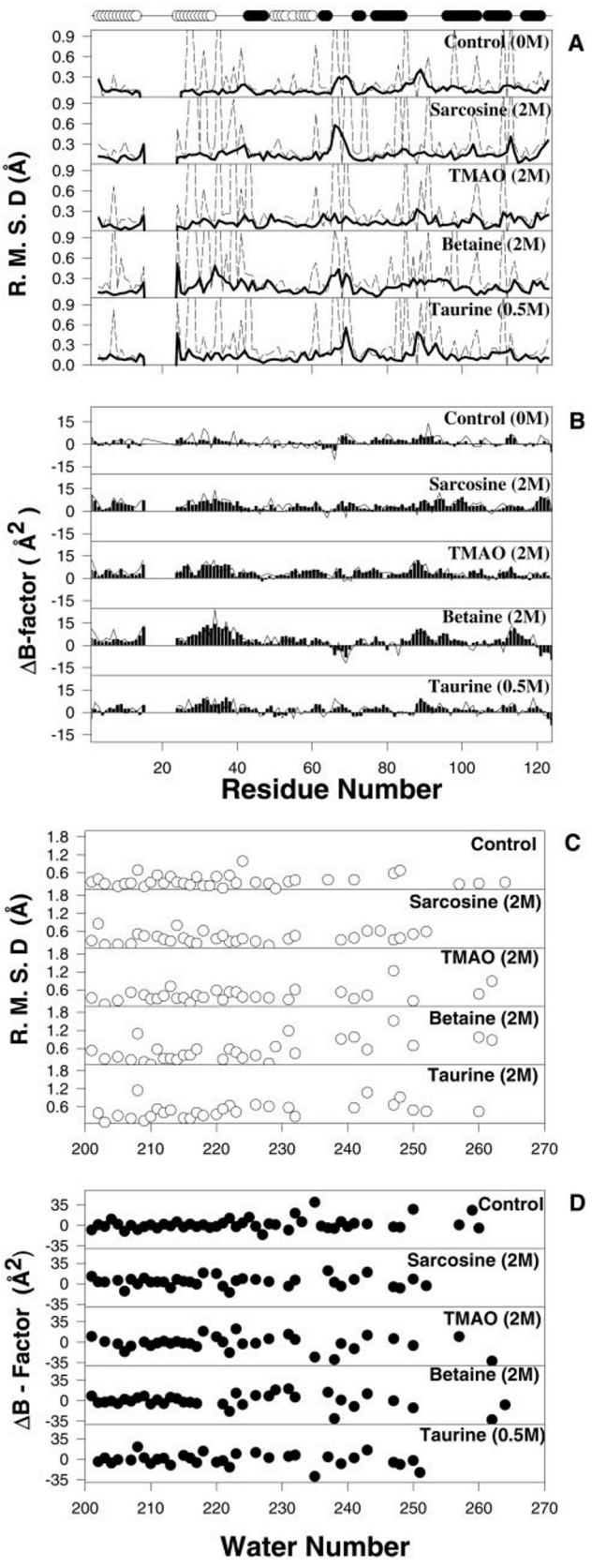

FIG. 4. **Effect of osmolytes on the crystal structure of RNase S.** The background error for r.m.s.d. and Δ*B*-factor plots was determined by comparison between the control structures obtained in the absence of osmolyte. *A*, r.m.s.d. plot for all osmolytes. MC and SC r.m.s.d. values are represented by *solid* and *dashed lines*, respectively. The large side-chain r.m.s.d. values are generally due to lack of density for side chains on the surface. The structure was superposed on its control structure before calculating the r.m.s.d. *B*, the restrained *B*-factor per residue for the control structure was subtracted from the corresponding *B*-factor of the structure of interest (osmolyte − control) to get the Δ*B*-factor plot. The *filled bars* indicate the MC Δ*B*-factors and the *lines* represent the SC Δ*B*-factors. The secondary structure representation on *top of the panel* indicates helices (○), β-strand (●), and loops/turns (−). *C*, r.m.s.d.; *D*, Δ*B*-factor plot for the crystallographic water molecules surrounding the osmolyte-soaked proteins. The r.m.s.d. and Δ*B*-factors were calculated as described above.

lower concentration than used solution. The crystals diffracted to high resolution in the presence of molar concentrations of osmolyte. Table II gives details of data collection and refinement for single crystals soaked in all four osmolytes and a control data set. The control data set was collected in stabilizing solution without any addition of osmolyte. The root mean square deviation (r.m.s.d.) plots for the osmolyte structure shows that there are no significant changes in the average main-chain (MC) and average side-chain (SC) positions compared with the control structure (Fig. 4*A*). The r.m.s.d. for MC for the osmolyte-soaked structures ranged from 0.14 to 0.16 Å and were similar to that of the control (0.12 Å). The differences in r.m.s.d. and *B*-factors in the control indicate the differences expected for redetermination of the same structure (19). The SC r.m.s.d. was in the range of 0.38 Å and was slightly more than that observed in the control (0.28 Å). The magnitude of the increases was much smaller than that seen when the structure is perturbed by 5 M urea (MC = 0.31 Å, SC = 0.63 Å (19)). The Δ*B*-factors show a small increase in all four osmolytes when compared with the control (Fig. 4*B*). The MC *B*-factors for the osmolyte structures are in the range 24–26 $Å^2$ and are slightly higher than that of the control (21 $Å^2$). This increase in *B*-factors is less than that seen in the case of RNase S perturbed by 5 M urea (30 $Å^2$) (19).

The osmolyte structures were compared with the control structure using the parameters of accessibility, depth, OS, and packing value (see "Experimental Procedures"). No significant changes were seen between the osmolyte structures and the control for the parameters accessibility, depth, and OS when compared at the residue level. The ΔMP of the osmolyte structures (relative to the control) was always positive. The osmolyte structures had a ΔMP of 0.0123, 0.0106, 0.0138, and 0.0064 for the sarcosine, betaine, TMAO, and taurine structures. In comparison, the ΔMP between two control structures was 0.0048. As an additional control, values of MP were measured for three cavity containing mutants (12), which were expected to have reduced packing density and negative values of ΔMP. As expected, the ΔMP for the mutants F8M, F8Nle, and F8A were −0.0024, −0.0026, and −0.0039, respectively. The positive ΔMP values for the crystal structures in the presence of osmolyte are consistent with a slight compaction of the native state in the presence the osmolyte. However, this small compaction is unlikely to be the source of increased stability, because the average ΔMP for five urea-soaked crystal structures of RNase S (19) was 0.011.

An analysis of water structure for all four osmolytes shows that there is no significant change in the number and position of the crystallographic waters (Fig. 4*B*) from the control structure. There are increases in the r.m.s.d. and scatter in the Δ*B*-factors (Fig. 4*B*) of water in the osmolyte crystal structures, but these changes are in the range of changes observed in the urea-soaked data sets (19). No density for additional water molecules as compared with that of those in the 0 M control or for osmolyte molecules was seen in any of the osmolyte-soaked structures. The Δ*B*-factor plots of the water structure around the protein indicate that the change in *B*-factors for the osmolyte-soaked structures is much less than that observed in the urea-soaked structures (Fig. 5 in Ref. 19). Water molecules

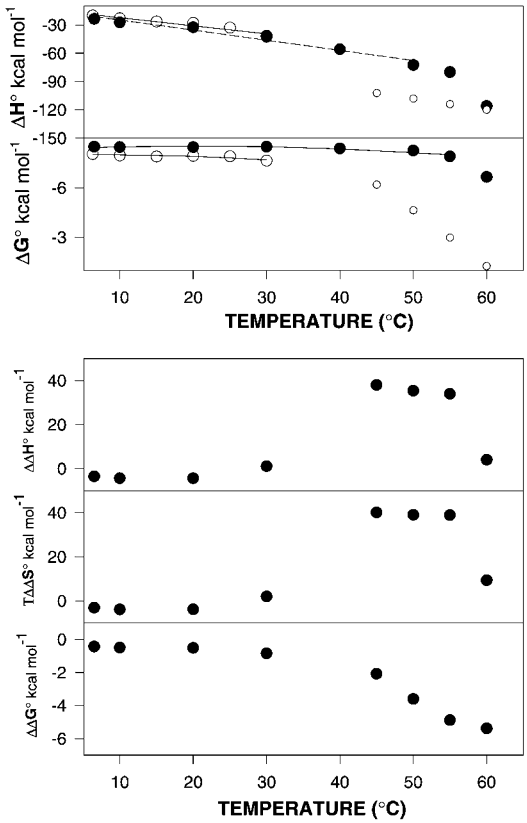

FIG. 5. **Temperature dependence of ΔH^0, ΔG^0 of the binding of S pep to S pro in the presence (*filled circles*) and absence (*empty circles*) of 6 M sarcosine.** The *smaller empty circles* represent data from DSC. The ΔH^0 values are fit to a *straight line* to derive the ΔC_p of binding. The *unbroken line* represents the ΔC_p fit over the temperature range 6–30 °C, whereas the *broken line* represents the fit for the range 6–50 °C in the presence of osmolyte. The *thin unbroken line* represents the ΔG^0 values fit to the van't Hoff equation as described previously (21) using parameters at 20 °C listed in Table IV.

#200 to #220 have almost the same *B*-factor as in the control structure. This data are in strong contrast to the urea-soaked crystal structures (19) where the waters had significant *B*-factor changes. These water molecules are the ones extensively hydrogen-bonded to the protein and form part of the first hydration shell. The waters in the sarcosine-soaked structure show minimal *B*-factor change relative to other osmolytes. The absence of bound osmolyte in the structures agrees with the notion that osmolytes are excluded from the protein surface as indicated by experiments by Timasheff's group (2, 40). Although it has been assumed that exclusion of osmolyte does not directly perturb the water structure directly around the protein (6, 41), this is the first direct experimental verification of this assumption.

Sarcosine Stabilizes the S Pro·S Pep Interaction—A complete thermodynamic analysis of S pep binding to S pro was done using titration calorimetry in the absence and presence of a single osmolyte, sarcosine, at a single concentration (6 M) at pH 5 (Table IV). Sarcosine was used because it stabilized RNase S and S pro to heat denaturation in a significant manner and also caused S pep to adopt a more compact conformation. Control titrations were done in buffer and in TMAO, an osmolyte which did not stabilize RNase S and S pro to a significant extent. At pH 5, there were problems of S pro sticking to the calorimetric cell, but we could collect data for TMAO at 2 M. Data for temperatures at and above 40 °C could not be collected for the control and TMAO titrations because of aggregation and binding of S pro (near its T_m) to the surface of the calorimetric cell. To get information on thermodynamic parameters at temperatures at 40 °C and above, the following procedure was adopted. Data for temperatures higher than 40 °C were measured from DSC studies on RNase S unfolding. ΔH_m, T_m, and ΔG^0 (T_m) vales measured for the unfolding of RNase S in buffer at pH 5 are 102 kcal mol^{-1}, 45 °C, and −6.19 kcal mol^{-1} and are in agreement with parameters measured in an earlier study in similar buffer conditions (22). A ΔC_p value of 1.2 kcal mol^{-1} K^{-1} (22) was assumed because the buffer conditions were similar. Stability data at temperatures above 45 °C were calculated using the above thermodynamic parameters using the van't Hoff equation as described previously (32). Because RNase S is a dissociating system, the ΔG^0 (T_m) is not equal to zero (22).

Aggregation of S pro was reduced in the presence of sarcosine. This factor combined with the stabilization of S pro and RNase S in the presence of sarcosine allowed collection of titration data to 60 °C. At this temperature the dissociation constant (K) was 2.3×10^{-4}, which is close to the limit of K_d (10^{-3}), which can be measured in a titration calorimeter. The S pep binding to S pro in sarcosine is tighter at all temperatures investigated (Table IV; Fig. 5) relative to its control. The ΔC_p was −0.85 and −0.72 kcal mol^{-1} K^{-1}, respectively, in the absence and presence of 6 M sarcosine, in the temperature range 6–30 °C. At temperatures higher than 30 °C, there is a significant increase in the magnitudes of ΔC_p and ΔH^0 of binding of S pep to S pro in the absence of osmolyte (21, 31). This increase results from the denaturation of free S pro at elevated temperatures. The binding reaction at temperatures below 30 °C is between folded S pep and folded S pro. At higher temperatures the binding occurs between unfolded S pep and unfolded S pro, and the enthalpy of folding of S pro constitutes a significant fraction of the total enthalpy of binding. In the presence of sarcosine, ΔH^0 increases linearly with temperature up to ~60 °C. This is consistent with the increase in T_m of S pro from 35.3 °C in the absence of sarcosine to 53.5 °C in 6 M sarcosine. Analysis of ΔH^0 as a function of T, over an extended temperature range, shows that the ΔC_p of binding in 6 M sarcosine is 1.1 kcal mol^{-1} K^{-1} and that ΔC_p is independent of temperature over a wide temperature range. Although this temperature independence is often assumed in calorimetric studies, the present data represent one of the few cases where it has been possible to verify this assumption.

DISCUSSION

Osmolyte stabilization of proteins is better understood today than when this phenomenon was first described (1, 7). Differential scanning calorimetry (DSC (3, 4, 42)), hydrogen exchange (43–45), folding kinetic studies (46), vapor phase osmometry (47, 48), densitometry (2, 8), and differential refractometry (8) have been used to dissect out the mechanism of osmolyte stabilization of proteins. Initial models of osmolyte stabilization focused on exclusion of osmolyte from the protein surface (2, 49) and preferential hydration of the native state (2). In addition to exclusion of osmolytes from the native state, osmolytes may also destabilize the unfolded state (8) by influencing the hydration profile of this state (4). Based on studies of the transfer of amino acid side chains and peptide backbone models from water to osmolyte solutions, Liu and Bolen (1995) showed that the ΔG^0_{tr} of the peptide backbone to osmolyte solutions was unfavorable. Hence, in the presence of osmolyte, the unfolded state (which has a greater accessible surface) should be destabilized relative to the native state. Recent evidence indicates that disordered and partially folded states can be induced to adopt a folded, native-like conformation in the presence of osmolytes (50–53). Models for osmolyte stabilization must also incorporate the compaction of unfolded states by

TABLE IV

Thermodynamic characterization of the binding of S pep to S pro in the absence and presence of molar osmolyte concentrations in 100 mM sodium chloride, 50 mM sodium acetate, pH = 5

Data from 45 °C to 60 °C for the binding of S pro to S pep in buffer has been measured using DSC. All other data points have been measured using titration calorimetry.

T	ΔH^0_{obs}	$K \times 10^{-6}$	ΔG^0	$T\Delta S^0$
°C	*kcal mol^{-1}*	*M^{-1}*	*kcal mol^{-1}*	
Buffer				
6.3	−20.2	1.93	−8.00	−12.20
10.0	−23.1	1.40	−7.96	−15.15
15.0	−26.6	0.96	−7.88	−18.71
20.0	−28.1	0.82	−7.93	−20.16
25.0	−33.1	0.62	−7.90	−25.19
30.0	−42.7	0.32	−7.63	−35.06
45.0	−102.0	0.05	−6.19	−95.81
50.0	−108.0	0.007	−4.64	−103.3
55.0	−114.0	0.0001	−2.99	−111.0
60.0	−120.0	0.0001	−1.26	−118.7
6 M sarcosine				
6.5	−23.7	4.21	−8.47	−15.28
10.0	−27.5	3.38	−8.46	−19.04
20.0	−32.5	2.00	−8.45	−24.04
30.0	−39.6	1.30	−8.48	−33.11
40.0	−56.0	0.70	−8.37	−47.62
50.0	−72.6	0.38	−7.25	−64.34
55.0	−80.0	0.18	−7.89	−72.10
60.0	−116.0	0.02	−6.64	−109.0
2 M betaine				
20.0	−31.7	0.88	−7.9	−23.8
30.0	−40.1	0.30	−7.6	−32.5
2 M TMAO				
10.0	−29.2	0.53	−7.41	−21.7
20.0	−31.6	0.30	−7.34	−24.2
30.0	−36.7	0.08	−6.80	−29.9

osmolytes (52, 53), the counteractive effect of urea (7, 8), and the effect osmolytes have on the aggregation state of proteins (54). Another observation that requires explanation is that often a given protein only shows enhanced stability in some osmolytes and not in others. The degree of stabilization does not necessarily correlate either qualitatively or quantitatively with values obtained from free energy of transfer studies. For example, RNase S is only stabilized to a significant degree in the presence of sarcosine and to a lesser extent by betaine and TMAO (Table III). In contrast transfer studies suggest that TMAO should have stronger stabilizing effects than sarcosine (52). The stability of bovine serum albumin is also greater in betaine than in TMAO. This was suggested to be due to greater exclusion of betaine from the protein surface (48). The temperature dependence of osmolyte-induced stabilization is also not well characterized. Recent data (55) suggest that stabilization only occurs at higher temperatures and not at room temperature, although large extrapolations of measured T_m values were involved in arriving at this conclusion. This observation is hard to explain on the basis of model compound ΔG^0_{tr} studies.

The S pro·S pep system is an ideal system to study the effects of osmolytes on protein stability for reasons discussed in the introduction. In the presence of a stabilizing osmolyte such as sarcosine, S pro and S pep are more structured than in its absence. In the presence of osmolyte, the S pro fragment appears to fold to a native-like structure with an increased near-UV-CD signal and is protected against proteolytic cleavage (Fig. 6). We denote this compact native-like state as the "O" state. The S pro O state is distinguished from the native state of unbound S pro by having part of the sequence (residues 38–124) being more compact under similar conditions of pH and temperature. The S pep is more compact (Fig. 6) in the presence of osmolyte but does not appear to be helical. At room temperature S pep binds more tightly to S pro in the presence of sarcosine than in its absence. Hence the value of $\Delta\Delta G^0 = \Delta G^0(6\ M) - \Delta G^0(0\ M)$ is negative. $\Delta\Delta G^0$ becomes more negative with increasing temperature, and the osmolyte-induced stabilization changes from being enthalpy-driven at room temperature to being entropy-driven at higher temperatures. The enhanced stabilization at higher temperatures is primarily due to osmolyte-induced stabilization of S pro in a native-like conformation.

The effects of osmolyte and temperature on the conformations of the bound and free components of RNase S are summarized in Table V: (i) At temperatures less than 30 °C binding occurs between folded S pro and unfolded S pep both in the presence and absence of 6 M sarcosine. (ii) The T_m values of S pro in the absence and presence of 6 M sarcosine are 36 and 53 °C, respectively. Hence, between 30 and 40 °C there is gradual unfolding of S pro in the absence of osmolyte, so binding occurs to a mixture of unfolded and folded S pro. At all temperatures above 45 °C, in the absence of osmolyte, binding occurs exclusively between S pep and unfolded S pro (Fig. 6). However, in the presence of osmolyte, at temperatures less than 50 °C binding occurs primarily between S pep and folded S pro. (iii) Between 50 and 60 °C, in the presence of sarcosine S, pep binds to a mixture of folded and unfolded S pro. At temperatures greater than 60 °C, binding occurs between S pep and unfolded S pro both in the presence and absence of osmolyte.

At temperatures below 30 °C, the enhanced binding in the presence of osmolyte is primarily due to enthalpic factors. The origin of this favorable enthalpic stabilization is unclear. In the temperature range of 30–55 °C the degree of osmolyte-induced stabilization increases substantially and is entropically driven. In the absence of osmolyte, S pep binds to unfolded S pro, whereas in the presence of osmolyte, S pep binds to folded S pro. Hence, in the absence of osmolyte, binding is coupled to an unfavorable entropy of folding. At temperatures above 55 °C, in

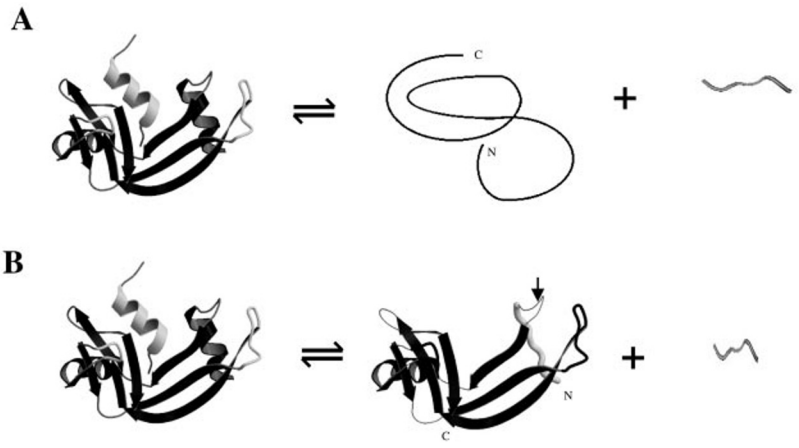

FIG. 6. **Schematic representation of the folded state of RNase S and its fragments in the presence and absence of sarcosine at 45 °C.** *A*, in the absence of sarcosine a major fraction of RNase S is dissociated into S pro and S pep. Both fragments are unfolded at this temperature. *B*, in the presence of sarcosine, S pro is folded and S pep shows increased compactness. The C-terminal part of S pro, S pro-(38–124), is protected against tryptic cleavage. The site of tryptic cleavage is indicated by an *arrow*.

TABLE V
Comparison of conformational state of RNase S and its fragments S pro and S pep as function of temperature in the presence and absence of 6 M sarcosine

T	0 M osmolyte		6 M sarcosine[a]	
	S pep	S pro	Unfolded	S pro
°C				
<30	Unfolded	Folded	Unfolded	Folded
30–45	Unfolded	Folded + unfolded	Unfolded	Folded
45–50	Unfolded	Unfolded	Unfolded	Folded
50–60	Unfolded	Unfolded	Unfolded	Folded + unfolded
>60	Unfolded	Unfolded	Unfolded	Unfolded

[a] Unfolded states in the presence of sarcosine are likely to be more compact than in its absence.

the presence of sarcosine, there is a substantial decrease in both binding affinity and the value of ΔH^0 (Table IV). This abrupt change in the magnitude of these two parameters is indicative of unfolding of unbound S pro. This was clearly established by earlier studies of the thermodynamics of binding of S pep to S pro as a function of temperature in the absence of osmolyte (21). For reasons that are currently unclear, there is a slight discrepancy of a few degrees in the apparent T_m of S pro inferred in this way relative to the value of 53.5 °C obtained from DSC studies in the presence of osmolyte. At temperatures above 60 °C, the unfolding of unbound S pro is complete, and at all higher temperatures binding occurs between S pep and unfolded S pro. Values of $\Delta\Delta G^0$ indicated in Fig. 5 show that there is a gradual increase in the magnitude of osmolyte-induced stabilization in the temperature range of 30 to 55 °C. There is only a small additional increase in the magnitude of $\Delta\Delta G^0$ between 55 and 60 °C.

Most previous studies of osmolyte-induced stabilization have focused on the exclusion of osmolytes from the protein surface and/or the unfavorable ΔG^0_{tr} of the unfolded state into osmolyte solutions. Osmolytes are thought to modulate protein stability primarily by affecting the stability and conformation of the unfolded state. Unfortunately, it is generally difficult to directly monitor the effect of osmolyte on the unfolded state, because unfolded states are populated to a very small extent under folding conditions. However, in the present case, because a bimolecular system is involved, it is possible to characterize osmolyte effects on the stability of the bound and free components, which are equivalent to the folded and unfolded states, respectively. It has also been possible to accurately characterize the temperature dependence of osmolyte-induced stabilization without having to resort to large extrapolations. A possible consequence of the unfavorable ΔG^0_{tr} of the unfolded state into osmolyte solutions is a compaction of the unfolded state so as to minimize the surface area in contact with osmolyte-containing solution. Some degree of compaction of unfolded state analogs has been previously observed (50, 52, 53), although it has not been possible to characterize the conformation of these states in any great detail.

In the present case there are at least two possible explanations for stabilization of RNase S by sarcosine. First, unfolded states of S pep and S pro are destabilized in the presence of the osmolyte. Second, the osmolyte is associated with conversion of unbound, unfolded S pro to a compact native-like state. This lessens the unfavorable entropic contribution associated with folding of S pro, prior to binding, in the absence of osmolyte (Figs. 5 and 6). The available data suggest that the second factor is the dominant one for the following reasons. Destabilization of the unfolded state should be correlated with ΔG^0_{tr} data for model compounds. In the case of model compounds, transfer studies show that ΔG^0_{tr} of the peptide backbone is higher for TMAO than for sarcosine. However, in the case of RNase S, sarcosine has a much greater stabilizing effect than does TMAO. In addition, only those osmolytes that stabilize the compact, native-like state of S pro appear to stabilize RNase S (Fig. 1, Table III). Finally, if destabilization of unfolded S pro by sarcosine was the primary cause for stabilization of RNase S, than it would be expected that there would be a significant increase in the magnitude of $\Delta\Delta G^0$ between 55 and 60 °C. This is the temperature range in which S pro unfolds. However, no such increase is seen (Fig. 5).

There have been several attempts to stabilize proteins by introducing mutations that decrease the conformational entropy of the native state (56, 57). These have met with limited success, either because of steric strain in the native state, enthalpic stabilization of the unfolded state or a decreased hydrophobic driving force for protein folding (58, 59). In contrast, osmolyte-induced unfolded states appear to be both compact and destabilized relative to the native state. The present work clearly shows that osmolytes do not perturb the folded structure of the native state or the water structure immediately around the protein. To obtain a clearer picture of the mechanism of osmolyte-induced stabilization, it is important to

characterize the temperature-dependent effects of osmolytes on the conformation, hydration, and stability of the unfolded state.

Acknowledgments—We thank Prof. Jayant Udgaonkar, National Center for Biological Sciences, Tata Institute for Fundamental Research, Bangalore, for use of the titration calorimeter. Computational facilities of the Supercomputer Education Research Center, the Interactive Graphics facility, and the Distributed Informatics Center, Indian Institute of Science have been utilized for this work. We also acknowledge use of the National Image Plate Facility and the Department of Biotechnology-sponsored Mass Spectrometry facility at the Molecular Biophysics Unit. We thank G. Chakshusmathi and K. Beena for helpful discussions.

REFERENCES

1. Yancey, P. H., Clark, M. E., Hand, S. C., Bowlus, R. D., and Somero, G. N. (1982) *Science* **217,** 1214–1222
2. Arakawa, T., and Timasheff, S. N. (1985) *Biophys. J.* **47,** 411–414
3. Santoro, M. M., Liu, Y., Khan, S. M., Hou, L. X., and Bolen, D. W. (1992) *Biochemistry* **31,** 5278–5283
4. Plaza del Pino, I. M., and Sanchez-Ruiz, J. M. (1995) *Biochemistry* **34,** 8621–8630
5. Liu, Y., and Bolen, D. W. (1995) *Biochemistry* **34,** 12884–12891
6. Xie, G., and Timasheff, S. N. (1997) *Protein Sci.* **6,** 211–221
7. Yancey, P. H., and Somero, G. N. (1979) *Biochem. J.* **183,** 317–323
8. Lin, T. Y., and Timasheff, S. N. (1994) *Biochemistry* **33,** 12695–12701
9. Kim, E. E., Varadarajan, R., Wyckoff, H. W., and Richards, F. M. (1992) *Biochemistry* **31,** 12304–12314
10. Chakshusmathi, G., Ratnaparkhi, G. S., Madhu, P. K., and Varadarajan, R. (1999) *Proc. Natl. Acad. Sci. U. S. A.* **96,** 7899–7904
11. Varadarajan, R., and Richards, F. M. (1992) *Biochemistry* **31,** 12315–12327
12. Ratnaparkhi, G. S., and Varadarajan, R. (2000) *Biochemistry* **39,** 12365–12374
13. Mitchinson, C., and Baldwin, R. L. (1986) *Proteins* **1,** 23–33
14. Kim, P. S., and Baldwin, R. L. (1984) *Nature* **307,** 329–334
15. Richards, F. M., and Wycoff, H. W. (1971) *The Enzymes* **4,** 647–806
16. Goldberg, J. M., and Baldwin, R. L. (1998) *Biochemistry* **37,** 2556–2563
17. Connelly, P. R., Varadarajan, R., Sturtevant, J. M., and Richards, F. M. (1990) *Biochemistry* **29,** 6108–6114
18. Goldberg, J. M., and Baldwin, R. L. (1998) *Biochemistry* **37,** 2546–2555
19. Ratnaparkhi, G. S., and Varadarajan, R. (1999) *Proteins* **36,** 282–294
20. Nadig, G., Ratnaparkhi, G. S., Varadarajan, R., and Vishveshwara, S. (1996) *Protein Sci.* **5,** 2104–2114
21. Thomson, J., Ratnaparkhi, G. S., Varadarajan, R., Sturtevant, J. M., and Richards, F. M. (1994) *Biochemistry* **33,** 8587–8593
22. Catanzano, F., Giancola, C., Graziano, G., and Barone, G. (1996) *Biochemistry* **35,** 13378–13385
23. Chakravarty, S., Mitra, N., Queitsch, I., Surolia, A., Varadarajan, R., and Dubel, S. (2000) *FEBS Lett.* **476,** 296–300
24. Fontana, A., Polverino de Laureto, P., De Filippis, V., Scaramella, E., and Zambonin, M. (1997) *Fold Des.* **2,** R17–R26
25. Allende, J. E., and Richards, F. M. (1962) *Biochemistry* **1,** 295–304
26. Ozer, I. (1998) *Anal. Biochem.* **264,** 199–203
27. Connolly, M. L. (1983) *Science* **221,** 709–713
28. Chakravarty, S., and Varadarajan, R. (1999) *Structure Fold. Des.* **7,** 723–732
29. Pattabiraman, N., Ward, K. B., and Fleming, P. J. (1995) *J. Mol. Recognit.* **8,** 334–344
30. Ratnaparkhi, G. S., Ramachandran, S., Udgaonkar, J. B., and Varadarajan, R. (1998) *Biochemistry* **37,** 6958–6966
31. Varadarajan, R., Connelly, P. R., Sturtevant, J. M., and Richards, F. M. (1992) *Biochemistry* **31,** 1421–1426
32. Ganesh, C., Shah, A. N., Swaminathan, C. P., Surolia, A., and Varadarajan, R. (1997) *Biochemistry* **36,** 5020–5028
33. Kurapkat, G., Kruger, P., Wollmer, A., Fleischhauer, J., Kramer, B., Zobel, E., Koslowski, A., Botterweck, H., and Woody, R. W. (1997) *Biopolymers* **41,** 267–287
34. Woody, R. W., and Dunker, K. A. (1990) Plenum Press, New York, pp. 109–158
35. Pflumm, M. N., and Beychock, S. (1969) *J. Biol. Chem.* **244,** 3973–3981
36. Ooi, T., Rupley, J. A., and Scheraga, H. A. (1963) *Biochemistry* **2,** 432–437
37. Persichetti, R. A., StClair, N. L., Griffith, J. P., Navia, M. J., and Margolin, A. L. (1994) *J. Am. Chem. Soc.* **117,** 2732–2737
38. Zelinski, T., and Waldmann, H. (1997) *Agnew Chem. Int. Ed. Engl.* **36,** 722–724
39. Maniken, M. W., and Fink, A. L. (1977) *Annu. Rev. Biophys. Bioeng.* **6,** 301–343
40. Timasheff, S. N. (1995) *Methods Mol. Biol* **40,** 253–269
41. Xie, G., and Timasheff, S. N. (1997) *Protein Sci.* **6,** 222–232
42. Knapp, S., Ladenstein, R., and Galinski, E. A. (1999) *Extremophiles* **3,** 191–198
43. Wang, A., Robertson, A. D., and Bolen, D. W. (1995) *Biochemistry* **34,** 15096–15104
44. Foord, R. L., and Leatherbarrow, R. J. (1998) *Biochemistry* **37,** 2969–2978
45. Knubovets, T., Osterhout, J. J., Connolly, P. J., and Klibanov, A. M. (1999) *Proc. Natl. Acad. Sci. U. S. A.* **96,** 1262–1267
46. Frye, K. J., and Royer, C. A. (1997) *Protein Sci.* **6,** 789–793
47. Zhang, W., Capp, M. W., Bond, J. P., Anderson, C. F., and Record, M. T., Jr. (1996) *Biochemistry* **35,** 10506–10516
48. Courtenay, E. S., Capp, M. W., Anderson, C. F., and Record, M. T. (2000) *Biochemistry* **39,** 4455–4471
49. Arakawa, T., Bhat, R., and Timasheff, S. N. (1990) *Biochemistry* **29,** 1924–1931
50. Baskakov, I., and Bolen, D. W. (1998) *J. Biol. Chem.* **273,** 4831–4834
51. Baskakov, I. V., Kumar, R., Srinivasan, G., Ji, Y. S., Bolen, D. W., and Thompson, E. B. (1999) *J. Biol. Chem.* **274,** 10693–10696
52. Qu, Y., Bolen, C. L., and Bolen, D. W. (1998) *Proc. Natl. Acad. Sci. U. S. A.* **95,** 9268–9273
53. Kendrick, B. S., Chang, B. S., Arakawa, T., Peterson, B., Randolph, T. W., Manning, M. C., and Carpenter, J. F. (1997) *Proc. Natl. Acad. Sci. U. S. A.* **94,** 11917–11922
54. Yang, D. S., Yip, C. M., Huang, T. H., Chakrabartty, A., and Fraser, P. E. (1999) *J. Biol. Chem.* **274,** 32970–32974
55. Anjum, F., Rishi, V., and Ahmad, F. (2000) *Biochim. Biophys. Acta* **1476,** 75–84
56. Burton, R. E., Hunt, J. A., Fierke, C. A., and Oas, T. G. (2000) *Protein Sci.* **9,** 776–785
57. Ratnaparkhi, G. S., Awasthi, S., Rani, P., Balaram, P., and Varadarajan, R. (2000) *Protein Eng.* **13,** 697–702
58. Dill, K. A. (1990) *Biochemistry* **29,** 7133–7155
59. Doig, A. J., and Williams, D. H. (1991) *J. Mol. Biol.* **217,** 389–398